

Photoluminescence studies of TM and RE doped oxides using diamond anvil cell

AGATA KAMIŃSKA

Institute of Physics, Polish Academy of Sciences, al. Lotników 32/46, 02-668 Warsaw, Poland;
e-mail: kaminska@ifpan.edu.pl

The present status of high-pressure research with the diamond anvil cell (DAC) is described, focusing mainly on use of this technique in optical spectroscopy. After a brief description of the history of the development of high-pressure measurements, the principles of DAC technique are described in more detail. Then different applications of this technique to high-pressure research are discussed, including optical spectroscopy, electrical measurements, X-ray diffractometry and other measurements. Results obtained for selected materials, with a view to illustrating the physics behind high-pressure phenomena, are presented and discussed. These include high-pressure luminescence studies of Cr³⁺ or Yb³⁺-doped lithium niobate crystal (LiNbO₃) as well as Cr³⁺ and Nd³⁺-doped lanthanum lutetium gallium garnet crystal (La₃Lu₂Ga₃O₁₂). Finally, the boundary of high-pressure spectroscopy usefulness is shown. The example of such a case is the study of Cr³⁺-doped MgO-2.5Al₂O₃ non-stoichiometric green spinel.

Keywords: diamond-anvil cells, high pressure, LiNbO₃, Cr³⁺ dopant, luminescence, garnet crystals, inhomogeneous broadening, Yb³⁺ ions, *f-d* transitions, spinel.

1. Introduction

The diamond anvil cell (DAC) technique has revolutionized research at pressures exceeding 10 kbar* both in terms of the range of hydrostatic pressures reached and the variety of other research techniques that can be employed to study various features of matter at high pressures.

The first to perform many pioneering high-pressure experiments was Percy Williams Bridgman. To this end he used self-constructed devices and obtained many interesting results (see [1–3] and references therein). He reached pressures of up to 100 kbar. His works attracted attention of scientific community to high pressure studies. In 1946, he received the Nobel Prize in Physics: he was awarded *for the invention of an apparatus to produce extremely high pressures, and for the discoveries he made therewith in the field of high pressure physics* (substantiation of Royal Academy of Sciences).

* Pressure is expressed in this article in kbar (kilobar) = 10³ bar; 1 bar = 10⁵ Nm⁻² (pascal) = 0.9869 atm. Another unit of pressure is GPa (gigapascal) = 10⁴ bar.

Improving further the construction of the devices which would enable obtaining pressures as high as possible brought about in 1959 the development of diamond anvil cell with optical access. This was done by the group of Charles E. Weir at the National Bureau of Standards (NBS) in Washington [4].

Although this cell was limited in pressure range and there was no reliable method of determining the pressure generated in the device, work at NBS and other laboratories continued on its development and applications because of the ease with which it could be employed to obtain high pressure data. Gradually, methods were elaborated for reaching higher and higher pressures and for measuring them, so DAC technique became a fine quantitative tool for modern physical research.

2. Principles of diamond anvil cell technique

The idea of the DAC is very simple [1–3, 5, 6]. As pressure is directly proportional to the applied force and inversely proportional to the area over which the force is applied, the pressure can be increased either by increasing the force or decreasing the area. The DAC makes use of the latter concept. This is the reason why diamond anvil cells are so small: the diameters of compressed surfaces of diamonds are in the range of 300–800 μm and the sample sizes: 50–150 μm . The gasket with the sample chamber is prepared by drilling a hole (100–300 μm in diameter) at the center of the indentation made by the anvil face on a metal foil. The gasket is seated on the lower diamond flat, then the sample and a pressure calibrator (most often, a ruby chip) are placed in the hole. This is followed by filling the hole with the fluid pressure transmitting medium (liquid argon, helium, xenon or methanol-ethanol mixture) and sealing by bringing the upper anvil on the gasket. Then the hydrostatic pressure inside the cell is increased by applying pressure to the diamonds (Fig. 1).

The gasket, apart from providing containment for the sample and the pressure medium, extrudes around the diamonds and acts as a supporting ring, preventing failure of the anvils due to concentration of stresses at the edges of the diamond anvil.

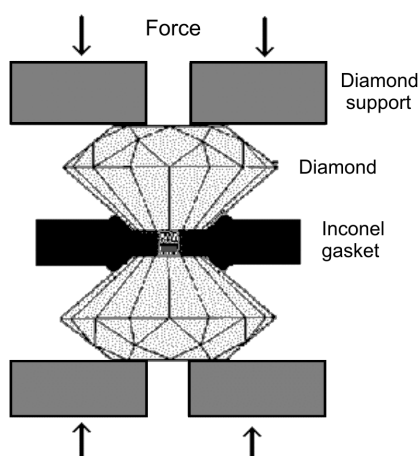


Fig. 1. Schematic diagram of the basic part of the diamond anvil cell.

The compressive strength and hardness of diamonds are extremely high, so they are able to support the required loads. In addition, they are transparent to the visible and IR light and to the X-ray radiation. The diamond anvil configuration enables optical access along the axis of the DAC, so the sample can be illuminated with the proper light and then many different experiments can be performed.

Up to now, various types of diamond anvil cells have been designed which differ in some construction details depending on experimental requirements. The main differences are the way of applying force and setting the proper alignment of diamonds (which have to be very precisely set parallel and coaxial). They also differ in sizes and the values of the highest pressures reached. However, the principles are the same in all types of diamond anvil cells [1–3, 5, 7–9].

3. Pressure calibration with ruby fluorescence

A standard method of determining the pressure generated inside the DAC is that with ruby fluorescence. A tiny chip of ruby 5–10 μm in dimension is placed in the pressure medium along the sample and luminescence is excited by either an argon-ion laser or any source of the strong light. The *R*-lines of ruby are quite narrow, intense, shift linearly with increasing pressure and broaden if the ruby experiences nonhydrostatic stresses. PIERMARINI *et al.* [10] showed that the pressure shift is linear up to 300 kbar. The linear scale holds good at any temperature down to 4.2 K and the pressure coefficient is exactly the same as that at room temperature.

From the results of ruby line shift as well as lattice parameter of Cu, Mo, Ag and Pt determined simultaneously and referring to isothermal equations of state derived from the shock-wave experiments, MAO *et al.* [11] concluded that there is a small nonlinearity in the pressure dependence of the wavelength shift of the *R* lines and that

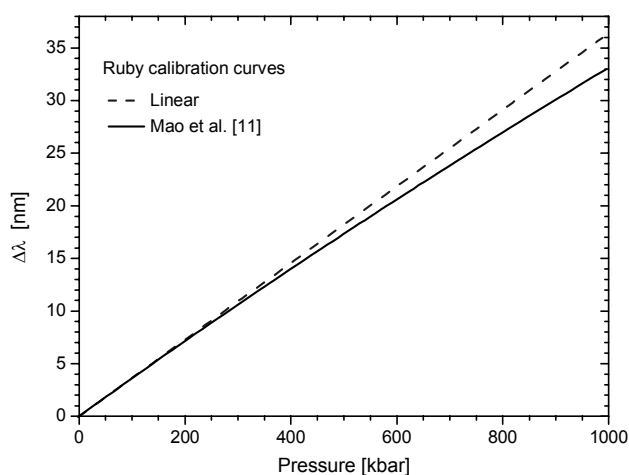


Fig. 2. Wavelength shift with pressure of the ruby fluorescence R_1 line. The pressure according to linear extrapolation is: $p(\text{kbar}) = 3.808[(\Delta\lambda/\lambda_0 + 1)^5 - 1]$; λ_0 – the wavelength at 1 atm (after [11]).

the linear scale underestimates the pressure, but this effect must be taken into account at pressures over 300 kbar. They determined proper correction coefficients which allow using ruby as a pressure calibrator up to megabar magnitudes (Fig. 2).

4. Applications of DAC technique

The DAC technique has really many features that are profitable as regards research applications. Apart from a relatively low price, miniature size, portability and compatibility with other apparatus it enables at present obtaining a broad range of hydrostatic and stable pressures (up to 6×10^6 atm) as well as temperatures – from liquid helium up to 6000 K [12–20]. With contemporary DACs a variety of sophisticated measurements can be performed on materials of microscopic dimensions.

Raman and Brillouin scattering studies and also powder or single-crystal X-ray diffraction studies are becoming routine investigations with the DAC. All types of diamond anvil cells are suited for powder diffraction work. However, single-crystal diffraction studies require specially modified constructions with wide conical apertures for the transmission of the diffracted X-rays over a wide angle. Furthermore, gases can be loaded into the gasket and then solidified as single crystals for the study of their structure, compressibilities and pressure-induced phase transitions [2].

DAC technique is also used to high pressure electrical measurements, although the problem of contacts needs to be solved. The four-lead arrangement is the most often used. Compression of materials induces changes in their electronic states connected with the crystallographic transformations to closer packed structures. A list of materials which undergo pressure induced semiconductor-to-metal and insulator-to-metal transitions is very long. One of the well-studied materials is the technologically critical silicon, which transforms at low temperatures at 120 kbar.

High pressure can also cause the superconducting transition temperature to elevate. This effect is attributed mainly to the increase in average phonon frequencies with applied pressure or in high-pressure phases.

Using DAC technique enables simulation of conditions like those in the earth mantle. In this way, various geochemical and geophysical studies can be performed. In addition, a new class of compounds impossible to obtain under normal conditions can be synthesized. They have the novel stoichiometry, such as $\text{He}(\text{N}_2)_{11}$, NeHe_2 , $\text{Ar}(\text{O}_2)_3$, $(\text{H}_2)_4(\text{O}_2)_3$. Their crystal structure and stoichiometry can be understood in terms of the efficiency with which the molecules and atoms can be packed.

BLOCK and PIERMARINI [1], JAYARAMAN [2] and HEMLEY and ASHCROFT [21] give detailed reviews of the aforementioned high pressure physical research.

5. Optical measurements

The most common measurements made under high pressures are these of optical absorption and luminescence. One of the first studies performed with the DAC were

the studies of pressure effects on infrared spectra of inorganic materials [4]. The high pressure luminescence studies allow us to observe transitions between direct (Γ) and indirect (L or X) minima and determine the shifts in the energy gap of many semiconductors [22–31].

Furthermore, this technique occurs to be a powerful tool for investigating the transition metal and rare earth luminescent centers in crystals. Application of high pressure reduces distances between a dopant ion and ligands, even up to a few per cent at relatively modest pressures. Thus, pressure increases considerably the crystal field strength experienced by the dopant ion, since it is approximately proportional to the inverse of the fifth power of the dopant ion–ligand distance. In this way, DAC allows one to continuously alter the crystal field strength experienced by the ions and to determine through luminescence measurements many important spectroscopic parameters, very difficult to measure with the help of other techniques. Especially sensitive to its crystal field surrounding are transition metal ions, whose d -electrons are less screened than inner f -shield electrons of the rare earth ions [32–52].

Another kind of optical measurements are reflectivity measurements. They are useful to derive information on the high-pressure changes of electronic structure of highly absorbing and metallic systems. Measurements of SmS, which undergoes a continuous $4f$ -electron delocalization and valence change with pressure, occurred to be very interesting. With increasing pressure the sample goes through a sequence of colour changes. Similar studies were performed with cesium, iodine, zinc sulfide, *etc.* (see [2] and references therein, [53, 54]).

6. Experimental results and discussion

The high-pressure measurements, the results of which are presented in this paper, were performed with the use of two different low temperature diamond anvil cells (Diacell Products MCDAC, Fig. 3). The diameters of compressed surfaces of diamonds are equal to 750 μm in the first and 450 μm in the second DAC. They enable attaining pressures up to 200 and 500 kbar, respectively. Argon was used as a pressure-transmitting medium. The DAC was mounted into an Oxford 1204 cryostat equipped with a temperature controller for low-temperature measurements. The R_1 -line ruby fluorescence was used for pressure calibration. The spectra were measured with the use of a GDM-1000 double grating monochromator equipped with a cooled photomultiplier (EMI 9684B) with S1-type cathode and an SR530 lock-in amplifier.

The decay kinetics of the luminescence was measured with use of a SR430 Multichannel Scaler.

6.1. Cr^{3+} in LiNbO_3

Lithium niobate (LNO) crystals remain of interest as far as applications and fundamental studies are concerned. The defect structure of those crystals is still one of the main subjects of research. The Cr^{3+} ions turned out to be a very good probe of

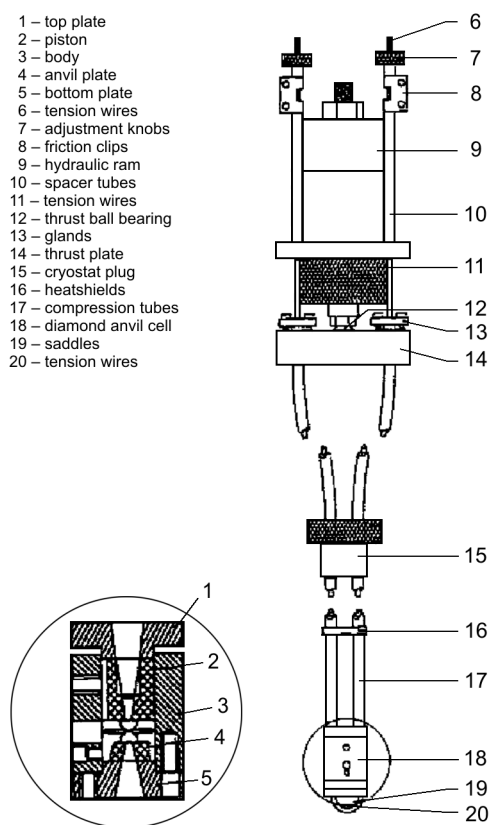


Fig. 3. Miniature cryogenic DAC and the drive mechanism (after [8]).

that structure since they substitute for both Li and Nb ions in LNO host. Occupancy of various sites and centers depends on concentration of chromium dopant, stoichiometry of the host and codoping with optically neutral ions, such as Mg or Zn.

The high-pressure spectroscopy occurred to be very successful in examining the Cr^{3+} ions in an octahedral crystal field environment because of their specific energy level structure. High-pressure application transforms the low-strength crystal field broadband and short-lived luminescence of chromium associated with the ${}^4T_2 \rightarrow {}^4A_2$ transitions into the high-strength crystal field sharp and long-lived luminescence lines related to the ${}^2E \rightarrow {}^4A_2$ transitions, which increases spectral resolution of the measurements and makes their characterization easier. The replacement of the broadband luminescence by sharp R -lines of Cr^{3+} ions with increasing pressure is presented in Fig. 4.

The high-pressure measurements show that in the $\text{LiNbO}_3:\text{Cr}$ crystals there are two main Cr^{3+} centers, denoted as center β and γ [42–44, 55] (see Fig. 5). Several studies performed with use of EPR and ENDOR techniques helped to identify these centers as Cr^{3+} ions in Li^+ sites [55, 56]. The dominating in this crystal is the γ center. However, in $\text{LiNbO}_3:\text{Mg,Cr}$ crystals, where the concentration of magnesium is increased above the definite threshold level (the value of the threshold depends on

the stoichiometry of the sample), there are three Cr^{3+} centers, center β , γ and δ (see Fig. 5). The additional low-strength crystal-field δ center dominates in this sample and it corresponds to Cr^{3+} ions in Nb^{5+} sites.

As can be seen in Fig. 5, the positions of R -lines change with the pressure – with increasing pressure they move towards lower energies, with the pressure coefficients

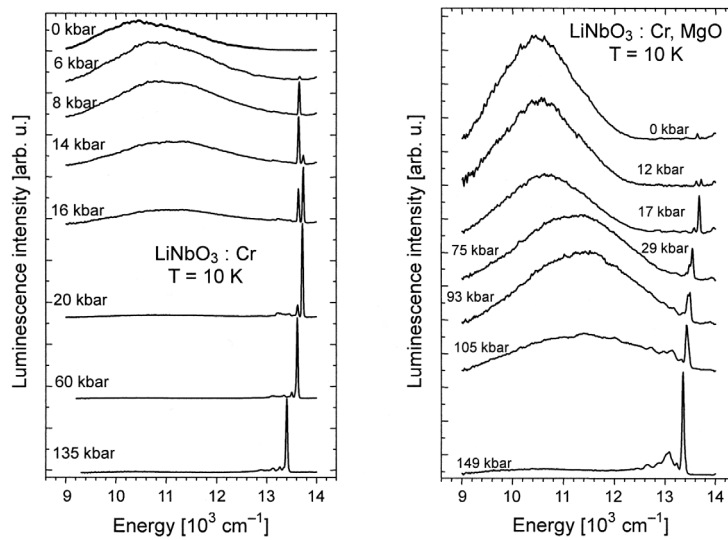


Fig. 4. Pressure dependence of the Cr^{3+} luminescence in near-stoichiometric $\text{LiNbO}_3:\text{Cr}$ (0.1% of Cr) and $\text{LiNbO}_3:\text{Cr}, \text{MgO}$ (0.1% of Cr, 0.2% of MgO) crystals.

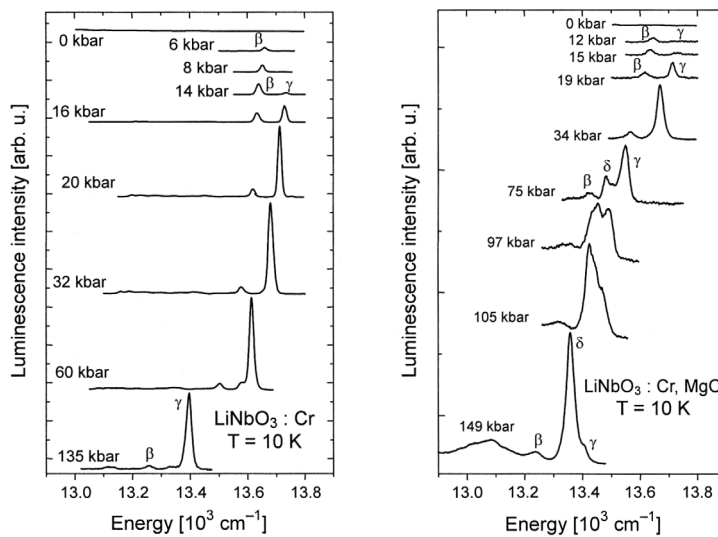


Fig. 5. Pressure dependence of the Cr^{3+} luminescence in near-stoichiometric $\text{LiNbO}_3:\text{Cr}$ (0.1% of Cr) and $\text{LiNbO}_3:\text{Cr}, \text{MgO}$ (0.1% of Cr, 0.2% of MgO) crystals in the region of the R -lines.

equal to -3.2 , -2.9 and -1.8 $\text{cm}^{-1}/\text{kbar}$ for the β , γ and δ centers, respectively. This is so-called nephelauxetic effect which is caused by the reduction of the bond lengths with pressure and, as a result, increasing the covalence of bonds between central ion and ligands and decreasing the interelectronic repulsion [57, 58].

The analysis of pressure-induced changes in the positions, widths, and decay times of electronic transitions enabled determination of some important spectroscopic parameters characterising chromium centers [44]. These are:

- the energy difference between the 2E and 4T_2 levels which describes the crystal field strength experienced by the chromium ions;
- the electron-lattice coupling energy (Huang–Rhys parameter);
- the value of the spin-orbit interaction.

Such analysis can be performed by fitting the theoretical diabatic model described in the literature [59] to the experimental results.

6.2. Cr^{3+} in $\text{La}_3\text{Lu}_2\text{Ga}_3\text{O}_{12}$

The large lattice parameters of lanthanum lutetium gallium garnet (LLGG) make them interesting, since the strength of the crystal field experienced by dopant ions in those crystals is lower than in other garnets.

High pressure experiments performed on the $\text{La}_3\text{Lu}_2\text{Ga}_3\text{O}_{12}:\text{Cr}^{3+}, \text{Nd}^{3+}$ crystal allowed us to establish that chromium ions occupy three groups of centers [47] (the Nd^{3+} ions were unintentional impurities). Nevertheless the problem of Cr^{3+} ions in this crystal differs from the problem of Cr-doped LNO. Lanthanum lutetium gallium garnet (LLGG) crystals are known to grow typically with a relatively large deviation from a stoichiometric composition. The real formula of our crystal is represented by $\{\text{La}_{1-x}\text{Lu}_x\}_3[\text{Lu}_{1-y}\text{Ga}_y]_2\text{Ga}_3\text{O}_{12}:\text{Cr}^{3+}, \text{Nd}^{3+}$, where: $x \approx 0.23$, $y \approx 0.07$, $\{\}$ describe the dodecahedral and $[\]$ – octahedral crystallographic sites. This nonstoichiometry causes inhomogenous broadening of luminescence lines, much larger than in the case of LNO. Furthermore, the nephelauxetic effect in LLGG occurred to be much weaker, which we ascribe to the fact that Cr^{3+} ions replace the Lu^{3+} ions of the same valence state, whereas in the LNO they replace either Li^+ or Nb^{5+} ions. This is manifested by the smaller value of pressure coefficient of R -lines in the LLGG crystal. On the other hand, because of weaker electron-lattice coupling of 4T_2 state we observe here the pronounced anticrossing effect connected with the quantum mixing of 4T_2 and 2E state. Because the pressure coefficients are equal to 11.0 $\text{cm}^{-1}/\text{kbar}$ for the 4T_2 state and -0.7 $\text{cm}^{-1}/\text{kbar}$ for the 2E state [47], as a result the peak positions of the R -lines first show blue shift with increasing pressure and then – red shift (see Fig. 6). The blue shift occurs in the region of the intermediate crystal field, near the crossing point of the theoretical energy levels of the 4T_2 and 2E state, where the participation of the 4T_2 state in the 2E state is the largest [40]. As the pressure is still raised, less and less of the 4T_2 character in R -lines is present and finally the luminescence of pure 2E state is observed with the shift to lower energy caused by the nephelauxetic effect.

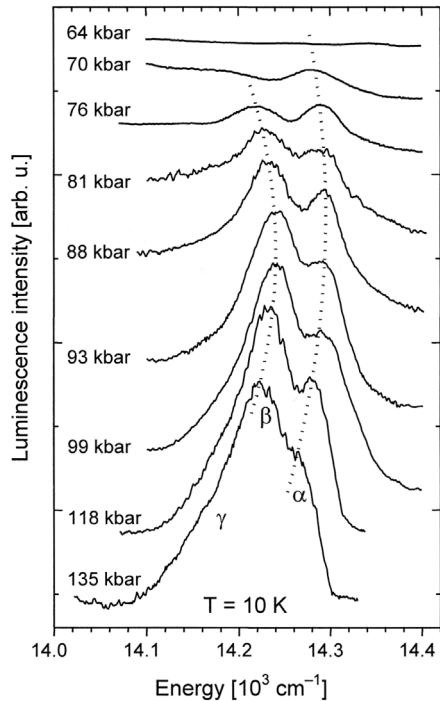


Fig. 6. Pressure dependence of the Cr^{3+} luminescence in the LLGG:Cr,Nd crystal at a temperature $T = 10$ K in the region of the R -lines. The broken lines mark the spectral positions of the R -line peaks.

The same type of anticrossing behaviour was observed and theoretically described by HÖMMERICH and BRAY [40, 41] in Cr^{3+} -doped gadolinium scandium gallium garnet (GSGG) where Cr^{3+} occupies sites of intermediate crystal field strength. This means that 2E and 4T_2 excited states are near the crossover point which results in their strong coupling and the pressure is here used to perturb the degree of the coupling.

6.3. Yb^{3+} in LiNbO_3

Yb^{3+} -doped materials are receiving increasing interest as solid state laser materials since the development of InGaAs laser diodes emitting near 980 nm, where the Yb^{3+} ions have a strong absorption peak. In particular, Yb doped LNO constitutes important subject of studies due to the demonstration of laser action at a wavelength of about 1 μm with the possibility of tuning and self-frequency doubling [60, 61].

Yb^{3+} ion has a very simple energy structure. It has only two states, ${}^2F_{7/2}$ fundamental and ${}^2F_{5/2}$ excited, separated by the energy of about 10000 cm^{-1} . The simple electronic structure implies the absence of parasitic effects such as excited-state absorption. Its special electronic configuration ($4f^{13}$) makes the $4f$ electrons less shielded than in other ions of the lanthanide series, and hence the electrons show a higher tendency to interact with the lattice and with neighbouring

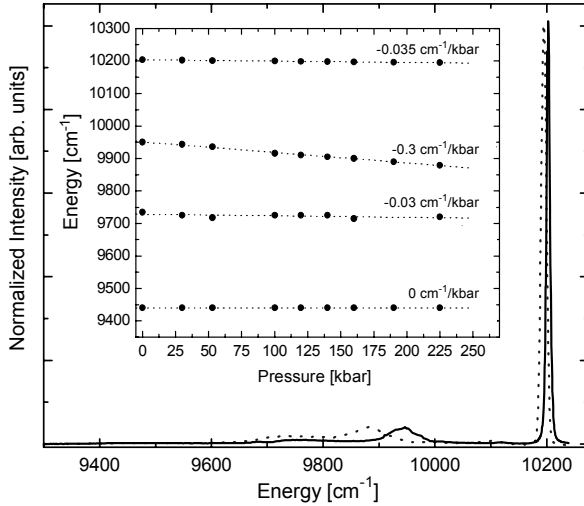


Fig. 7. Emission spectra associated with the ${}^2F_{5/2} \rightarrow {}^2F_{7/2}$ transitions of Yb^{3+} ion in $\text{LiNbO}_3:\text{Yb}(4\%)$ under excitation by c.w. Ti:sapphire laser tuned to 955 nm at a temperature $T = 10$ K. Solid line: ambient pressure, dotted line: 225 kbar. The inset shows the energy shifts of the transitions with pressure. For the clearness of the figure the intensity of the spectrum in the range of 9300–10170 cm^{-1} has been multiplied by 10.

ions, which is a prerequisite for cooperative interactions and the vibronic broadening observed in a variety of Yb^{3+} activated systems.

In principle, the electric-dipole transitions between the ${}^2F_{7/2}$ and ${}^2F_{5/2}$ states of Yb^{3+} ion are parity-forbidden and magnetic-dipole transitions should play an important role in the de-excitation of the excited ${}^2F_{5/2}$ state. However, in this crystal electric-dipole transitions appeared to be dominating.

Some admixture of another electronic configuration to the pure $4f$ one can perturb the energy states of Yb^{3+} and allow the electric-dipole transitions. For investigation of the role of various mechanisms responsible for relaxation of these transitions in the system of Yb^{3+} doped LiNbO_3 crystals the high-pressure measurements of the luminescence spectra and decay kinetics of the luminescence were performed.

Figure 7 presents the luminescence spectra of $\text{LiNbO}_3:\text{Yb}(4\%)$ crystal at ambient pressure and 225 kbar under excitation at the ${}^2F_{7/2}(0) \rightarrow {}^2F_{5/2}(1)$ transition [52]. As observed, the pressure application changes the spectra very slightly. As shown in the figure inset, most of the emission lines show a very small red shift with pressure. The results show that the crystal field splittings of the ${}^2F_{5/2}$ and ${}^2F_{7/2}$ ($4f^{13}$) states are not significantly affected in the range of applied pressure.

In contrast, the influence of pressure on the decay kinetics of the ${}^2F_{5/2}$ upper state of Yb^{3+} is highly pronounced. Figure 8 shows the pressure dependence of the luminescence decay times of the ${}^2F_{5/2}(0')$ level of the $\text{LiNbO}_3:\text{Yb}^{3+}(4\%)$ crystal, measured at emission wavelength of the ${}^2F_{5/2}(0') \rightarrow {}^2F_{7/2}(0)$ transition (*i.e.*, at

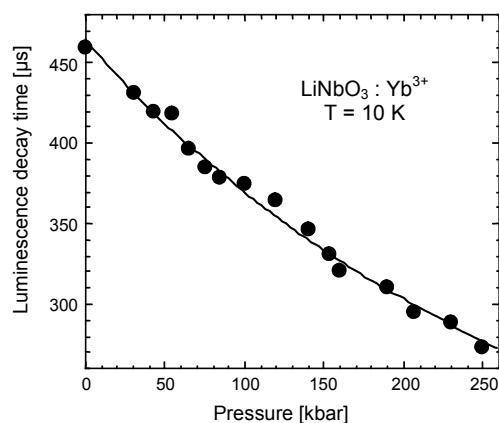


Fig. 8. Pressure dependence of the luminescence decay times of the ${}^2F_{5/2} \rightarrow {}^2F_{7/2}$ transitions of the Yb^{3+} ion in $\text{LiNbO}_3:\text{Yb}(4\%)$ crystal at a temperature $T = 10$ K. Points: experiment; line: theoretical fit (see the text).

a wavelength of about 980 nm and slightly longer at higher pressures). They were exponential for each measured pressure. As expected, similar results were obtained when monitoring the luminescence decay times at the other emission lines.

The luminescence decay times decrease from 458 μs at ambient pressure down to about 270 μs at a pressure of 250 kbar. The same results were observed in the sample with lower Yb content (1 at.%) and for different wavelength of measurements within the Yb^{3+} emission spectrum. This evidences that possible nonradiative de-excitation channels, such as energy transfer or energy diffusion are not affected by applying pressure at the given temperature and pressure range. In fact, the observed pressure-dependence lifetime reduction can be considered as a single-ion effect, since it is independent of concentration. Additionally, the emission intensity does not undergo significant changes which could be associated with a fluorescence quenching. Thus, the low temperature lifetime values obtained can be considered as the radiative lifetime values for measured pressure range.

Considering the enhancement of electric-dipole transitions in Yb^{3+} ions doped to LiNbO_3 crystal we should take into account the mixing of the $5d$ electronic orbitals into a pure $4f$ configuration as a mechanism of relaxation of the electric dipole selection rules. The effect of mixing the $4f^{13}$ and $4f^{12}5d^1$ electronic configurations depends on their energy separation, which decreases with pressure. The energy of the $5d$ electrons strongly depends on the crystal environment since $5d$ orbitals are not screened, in contrast to the $4f$ ones, and may change by tens of thousands of wavenumbers from one compound to another. Thus the admixture of the electric-dipole transition probability to the decay probability of the ${}^2F_{5/2}$ state of the $4f^{13}$ configuration increases with pressure and the decay time of the ${}^2F_{5/2} \rightarrow {}^2F_{7/2}$ transitions decreases.

The electric-dipole transitions can also occur as a result of the interaction of the dopant ion with a non-centrosymmetric crystal field. The trigonal distortion

of the crystal lattice increases with pressure causing an increase of the radiative transition probability as pressure directly influences the odd-parity potential by changing the Yb–O distances and changing the c/a lattice parameters ratio. The origin of these distortions is structural and it is not related to pressure non-hydrostaticity (see [52] and references therein).

In fact, the second effect gives the major contribution to electric-dipole transitions within the $4f$ shell. We fit to our experimental the data theoretical model [52] which takes into account both the decrease of the energy of the $4f^{12}5d^1$ level with pressure and changes in the value of the coupling coefficient, associated with the changes in the trigonal distortion with pressure (see Fig. 8). Numerical analysis of the results obtained shows that the decrease of the decay time of ${}^2F_{5/2} \rightarrow {}^2F_{7/2}$ transition of Yb^{3+} ion with increasing pressure is mainly determined by the variation of the odd parity crystal field parameter with pressure. It has been numerically checked that it is impossible to obtain such dependence without taking into account pressure changes of this parameter and obtain reasonable values of the remaining parameters at the same time.

The importance of the changes in the trigonal distortion on the observed increase of the radiative transition probability has been confirmed by our last high-pressure measurements of the gadolinium gallium garnet crystal doped with the Yb^{3+} ions. This crystal is cubic and here we observe only very small decrease of decay time with pressure. For a more detailed description of the problem further studies are under way.

6.4. Cr^{3+} in $\text{MgO-2.5Al}_2\text{O}_3$ synthetic spinel

It is known that synthetic spinels exhibit large disorder compared to natural spinels and that nonstoichiometry strongly contributes to this disorder. Chromium ions in $\text{MgO-2.5Al}_2\text{O}_3$ have been found to occupy several sites of various symmetries, however different authors have found different numbers of these sites: from 2 to 25 [62–66]. This discrepancy is associated with the complicated nature of the luminescence which consists of a broadband in the infrared region and several relatively sharp lines with the full-width at half-of-maximum (FWHM) in the range from 150 to 500 cm^{-1} , whose intensity in addition strongly depends on excitation wavelength.

For those reasons, as well as in the case of chromium doped LNO or LLGG crystals, we performed a series of high-pressure measurements in order to transform the low-strength crystal field broadband and short-lived luminescence of chromium ions into the high-strength crystal field sharp and long-lived luminescence and to increase in this way the spectral resolution of measurements [48]. However, as is shown in Fig. 9, very large inhomogenous broadening due to large crystallographic disorder does not allow us to obtain any new and unambiguous information on the multicenter structure of chromium dopant. The results of high-pressure luminescence and decay times of the luminescence measurements show only that there are four major groups of Cr^{3+} centers in the crystal. Two of these groups (α and β) are created by the strong

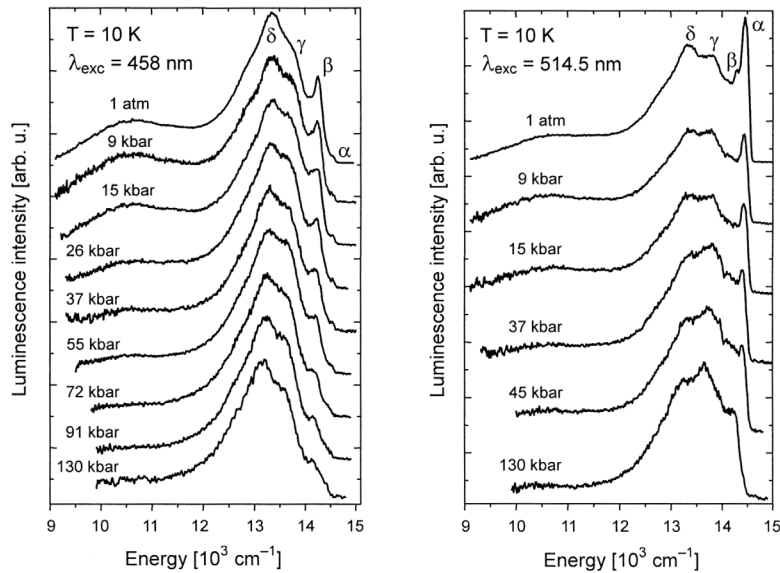


Fig. 9. Pressure dependence of the Cr^{3+} luminescence in non-stoichiometric green spinel $\text{MgO-2.5Al}_2\text{O}_3$ at a temperature $T = 10$ K, excited by the 448 and 514.5 nm Ar^+ laser line.

crystal field centers, whereas two others (δ and γ) – by the intermediate crystal field centers. Due to large inhomogeneous broadening some of the Cr^{3+} ions in δ and γ sites experience low crystal field at ambient pressure contributing to the broadband luminescence.

The large disorder present in this type of spinel makes it impossible to judge whether additional Cr^{3+} sites of smaller concentration can or cannot be found there.

7. Concluding remarks

The DAC technique can provide a lot of information either impossible or difficult to obtain in other ways and this is the main reason for still increasing interest in such a kind of research into the various fields of science. The full list of applications of DAC technique has by no means been exhausted. The present paper gives the basic review of the possibilities it offers as well as some selection of interesting results and physical phenomena which can be observed using this technique. A detailed description of DAC application and results obtained is presented in refereed papers.

Acknowledgements – The author thanks very much Professor A. Suchocki from the Institute of Physics of the Polish Academy of Sciences, Warsaw, Poland, for cooperation and helpful discussions, and M. Grinberg from the Institute of Experimental Physics of Gdańsk University, Poland, and S.W. Biernacki from the Institute of Physics of the Polish Academy of Sciences, Warsaw, Poland, for

elaborating theoretical models. Acknowledgement is also made to the cooperation with L. Arizmendi, L. Bausa and M. Ramirez from Departamento de Fisica de Materiales, Universidad Autonoma de Madrid, Spain.

References

- [1] BLOCK S., PIERMARINI G., *The diamond cell stimulates high-pressure research*, Physics Today **29**(9), 1976, pp. 44–7.
- [2] JAYARAMAN A., *Diamond anvil cell and high-pressure physical investigations*, Reviews of Modern Physics **55**(1), 1983, pp. 65–108.
- [3] JAYARAMAN A., *Ultrahigh pressures*, Review of Scientific Instruments **57**(6), 1986, pp. 1013–31.
- [4] WEIR C.E., LIPPINCOTT E.R., VAN VALKENBURG A., BUNTING E.N., Journal of Research for the National Bureau of Standards A **63**, 1959, p. 55.
- [5] DUNSTAN D.J., SPAIN I.L., *Technology of diamond anvil high-pressure cells. I. Principles, design and construction*, Journal of Physics E: Scientific Instruments **22**(11), 1989, pp. 913–23.
- [6] SPAIN I.L., DUNSTAN D.J., *The technology of diamond anvil high-pressure cells. II. Operation and use*, Journal of Physics E: Scientific Instruments **22**(11), 1989, pp. 923–33.
- [7] KELLER R., HOLZAPFEL W.B., *Diamond anvil device for X-ray diffraction on single crystals under pressures up to 100 kilobar*, Review of Scientific Instruments **48**(5), 1977, pp. 517–23.
- [8] DUNSTAN D.J., SCHERRER W., *Miniature cryogenic diamond-anvil high-pressure cell*, Review of Scientific Instruments **59**(4), 1988, pp. 627–30.
- [9] SILVERA I.F., WIJNGAARDEN R.J., *Diamond anvil cell and cryostat for low-temperature optical studies*, Review of Scientific Instruments **56**(1), 1985, pp. 121–4.
- [10] PIERMARINI G.J., BLOCK S., BARNETT J.D., FORMAN R.A., *Calibration of the pressure dependence of the R_1 ruby fluorescence line to 195 kbar*, Journal of Applied Physics **46**(6), 1975, pp. 2774–80.
- [11] MAO H.K., BELL P.M., SHANER J.W., STEINBERG D.J., *Specific volume measurements of Cu, Mo, Pd, and Ag and calibration of the ruby R_1 fluorescence pressure gauge from 0.06 to 1 Mbar*, Journal of Applied Physics **49**(6), 1978, pp. 3276–83.
- [12] RUOFF A.L., WANAGEL J., *High pressures on small areas*, Science **198**(4321), 1977, pp. 1037–8.
- [13] GOLOPENTIA D.A., RUOFF A.L., *Apparatus for high-pressure and low-temperature experiments*, Review of Scientific Instruments **52**(2), 1981, pp. 235–8.
- [14] RUOFF A.L., XIA H., LUO H., VOHRA Y.K., *Miniaturization techniques for obtaining static pressures comparable to the pressure at the center of the Earth: X-ray diffraction at 416 GPa*, Review of Scientific Instruments **61**(12), 1990, pp. 3830–3.
- [15] RUOFF A.L., LUO H., VOHRA Y.K., *The closing diamond anvil optical window in multimegabar research*, Journal of Applied Physics **69**(9), 1991, pp. 6413–6.
- [16] RUOFF A.L., LUO H., *Pressure strengthening: a possible route to obtaining 9 Mbar and metallic diamonds*, Journal of Applied Physics **70**(4), 1991, pp. 2066–70.
- [17] RUOFF A.L., LUO H., VANDERBORGH C., VOHRA Y.K., *Generating near-earth-core pressures with type-IIa diamonds*, Applied Physics Letters **59**(21), 1991, pp. 2681–2.
- [18] CHRISTENSEN N.E., RUOFF A.L., RODRIGUEZ C.O., *Pressure strengthening: a way to multimegabar static pressures*, Physical Review B: Condensed Matter **52**(13), 1995, pp. 9121–4.
- [19] RUOFF A.L., RODRIGUEZ C.O., CHRISTENSEN N.E., *Elastic moduli of tungsten to 15 Mbar, phase transition at 6.5 Mbar, and rheology to 6 Mbar*, Physical Review B: Condensed Matter **58**(6), 1998, pp. 2998–3002.
- [20] AKELLA J., *The diamond anvil cell: probing the behavior of metals under ultrahigh pressures*, Science and Technology Review, March 1996, pp. 17–27.
- [21] HEMLEY R.J., ASHCROFT N.W., *The revealing role of pressure in the condensed matter sciences*, Physics Today **51**(8), 1998, pp. 26–32.

- [22] MÜLLER H., TROMMER R., CARDONA M., VOGL P., *Pressure dependence of the direct absorption edge of InP*, Physical Review B: Condensed Matter **21**(10), 1980, pp. 4879–83.
- [23] VENKATESWARAN U., CHANDRASEKHAR M., CHANDRASEKHAR H.R., VOJAK B.A., CHAMBERS F.A., MEESE J.M., *High-pressure studies of GaAs-Ga_{1-x}Al_xAs quantum wells of widths 26 to 150 Å*, Physical Review B: Condensed Matter **33**(12), 1986, pp. 8416–23.
- [24] DI HONG R., JENKINS D.W., REN S.Y., DOW J.D., *Hydrostatic-pressure dependencies of deep impurity levels in zinc-blende semiconductors*, Physical Review B: Condensed Matter **38**(17), 1988, pp. 12549–55.
- [25] PERLIN P., TRZECIAKOWSKI W., LITWIN-STASZEWSKA E., MUSZALSKI J., MICOVIC M., *The effect of pressure on the luminescence from GaAs/AlGaAs quantum wells*, Semiconductor Science and Technology **9**(12), 1994, pp. 2239–46.
- [26] KIM S., HERMAN I.P., TUCHMAN J.A., DOVERSPIKE K., ROWLAND L.B., GASKILL D.K., *Photoluminescence from wurtzite GaN under hydrostatic pressure*, Applied Physics Letters **67**(3), 1995, pp. 380–2.
- [27] AKAMARU H., ONODERA A., ENDO T., MISHIMA O., *Pressure dependence of the optical-absorption edge of AlN and graphite-type BN*, Journal of the Physics and Chemistry of Solids **63**(5), 2002, pp. 887–94.
- [28] SUSKI T., TEISSEYRE H., LEPKOWSKI S.P., PERLIN P., KITAMURA T., ISHIDA Y., OKUMURA H., CHICHIBU S.F., *Different pressure coefficients of the light emission in cubic and hexagonal InGaN/GaN quantum wells*, Applied Physics Letters **81**(2), 2002, pp. 232–4.
- [29] LI S.X., WU J., HALLER E.E., WALUKIEWICZ W., SHAN W., LU H., SCHAFF W.J., *Hydrostatic pressure dependence of the fundamental bandgap of InN and in-rich group III nitride alloys*, Applied Physics Letters **83**(24), 2003, pp. 4963–5.
- [30] ANCEAU S., LEFEBVRE P., SUSKI T., LEPKOWSKI S.P., TEISSEYRE H., DMOWSKI L.H., KONCZEWICZ L., KAMIŃSKA A., SUCHOCKI A., HIRAYAMA H., AOYAGI Y., *Surprisingly low built-in electric fields in quaternary AlInGaN heterostructures*, Physica Status Solidi A **201**(2), 2004, pp. 190–4.
- [31] FRANSEN G., KAMIŃSKA A., SUSKI T., SUCHOCKI A., KAZLAUSKAS K., TAMULAITIS G., ZUKAUSKAS A., CZARNECKI R., TEISSEYRE H., PERLIN P., LESZCZYŃSKI M., BOĆKOWSKI M., GRZEGORY I., GRANDJEAN N., *Observation of localization effects in InGaN/GaN quantum structures by means of the application of hydrostatic pressure*, Physica Status Solidi B **241**(14), 2004, pp. 3285–92.
- [32] KOTTKE T., WILLIAMS F., *Pressure dependence of the alexandrite emission spectrum*, Physical Review B: Condensed Matter **28**(4), 1983, pp. 1923–7.
- [33] DOLAN J.F., KAPPERS L.A., BARTRAM R.H., *Pressure and temperature dependence of chromium photoluminescence in K₂NaGaF₆:Cr³⁺*, Physical Review B: Condensed Matter **33**(10), 1986, pp. 7339–41.
- [34] EGGERT J.H., GOETTEL K.A., SILVERA I.F., *Ruby at high pressure. I. Optical line shifts to 156 GPa*, Physical Review B: Condensed Matter **40**(8), 1989, pp. 5724–32.
- [35] EGGERT J.H., GOETTEL K.A., SILVERA I.F., *Ruby at high pressure. II. Fluorescence lifetime of the R line to 130 GPa*, Physical Review B: Condensed Matter **40**(8), 1989, pp. 5733–8.
- [36] DUCLOS S.J., VOHRA Y.K., RUOFF A.L., *Pressure dependence of the ⁴T₂ and ⁴T₁ absorption bands of ruby to 35 GPa*, Physical Review B: Condensed Matter **41**(8), 1990, pp. 5372–81.
- [37] WAMSLEY P.R., BRAY K.L., *The effect of pressure on the luminescence of Cr³⁺:YAG*, Journal of Luminescence **59**(1–2), 1994, pp. 11–7.
- [38] FREIRE P.T.C., PILLA O., LEMOS V., *Pressure-induced level crossing in KZnF₃:Cr³⁺*, Physical Review B: Condensed Matter **49**(13), 1994, pp. 9232–5.
- [39] WAMSLEY P.R., BRAY K.L., *The effect of pressure on energy transfer in Cr³⁺:Tm³⁺:YAG*, Journal of Luminescence **63**(1–2), 1995, pp. 31–9.
- [40] HÖMMERICH U., BRAY K.L., *Direct observation of anticrossing behavior in a luminescent Cr³⁺-doped system*, Physical Review B: Condensed Matter **51**(13), 1995, pp. 8595–8.

- [41] HÖMMERICH U., BRAY K.L., *High-pressure laser spectroscopy of $Cr^{3+}:Gd_3Sc_2Ga_3O_{12}$ and $Cr^{3+}:Gd_3Ga_5O_{12}$* , Physical Review B: Condensed Matter **51**(18), 1995, pp. 12133–41.
- [42] KAMIŃSKA A., DMOCHOWSKI J.E., SUCHOCKI A., GARCIA-SOLE J., JAQUE F., ARIZMENDI L., *Luminescence of $LiNbO_3:MgO,Cr$ crystals under high pressure*, Physical Review B: Condensed Matter **60**(11), 1999, pp. 7707–10.
- [43] KAMIŃSKA A., SUCHOCKI A., GRINBERG M., GARCIA-SOLE J., JAQUE F., ARIZMENDI L., *High-pressure spectroscopy of $LiNbO_3:MgO,Cr^{3+}$ crystals*, Journal of Luminescence **87–89**, 2000, pp. 571–3.
- [44] KAMIŃSKA A., SUCHOCKI A., ARIZMENDI L., CALLEJO D., JAQUE F., GRINBERG M., *Spectroscopy of near-stoichiometric $LiNbO_3:MgO,Cr$ crystals under high pressure*, Physical Review B: Condensed Matter **62**(16), 2000, pp. 10802–11.
- [45] BUNGENSTOCK C., TRÖSTER T., HOLZAPFEL W.B., *Effect of pressure on free-ion and crystal-field parameters of Pr^{3+} in $LOCl$ ($L=La, Pr, Gd$)*, Physical Review B: Condensed Matter **62**(12), 2000, pp. 7945–55.
- [46] SHEN Y., RIEDENER T., BRAY K.L., *Effect of pressure and temperature on energy transfer between Cr^{3+} and Tm^{3+} in $Y_3Al_5O_{12}$* , Physical Review B: Condensed Matter **61**(17), 2000, pp. 11460–71.
- [47] KAMIŃSKA A., KACZOR P., DURYGIN A., SUCHOCKI A., GRINBERG M., *Low-temperature high-pressure spectroscopy of lanthanum lutetium gallium garnet crystals doped with Cr^{3+} and Nd^{3+}* , Physical Review B: Condensed Matter and Materials Physics **65**(10), 2002, pp. 104106/1–8.
- [48] KAMIŃSKA A., SUCHOCKI A., GOŚCIŃSKI K., DOBACZEWSKI L., DEREŃ P.J., STRĘK W., *High-pressure spectroscopy of Cr^{3+} doped $MgO-2.5Al_2O_3$ non-stoichiometric green spinel*, Journal of Alloys and Compounds **341**, 2002, pp. 193–6.
- [49] KAMIŃSKA A., ARIZMENDI L., BARCZ A., ŁUSAKOWSKA E., SUCHOCKI A., *Cr^{3+} ions in hydrogenated and proton exchanged lithium niobate crystals*, Physica Status Solidi A **201**(2), 2004, pp. 298–303.
- [50] GRYK W., KUKLIŃSKI B., GRINBERG M., MALINOWSKI M., *High pressure spectroscopy of Pr^{3+} in $LiNbO_3$* , Journal of Alloys and Compounds **380**(1–2), 2004, pp. 230–4.
- [51] GRYK W., DYL D., RYBA-ROMANOWSKI W., GRINBERG M., *Spectral properties of $LiTaO_3:Pr^{3+}$ under high hydrostatic pressure*, Journal of Physics: Condensed Matter **17**(35), 2005, pp. 5381–95.
- [52] RAMIREZ M., BAUSA L., BIERNACKI S.W., KAMIŃSKA A., SUCHOCKI A., GRINBERG M., *Influence of hydrostatic pressure on radiative transition probability of the intrashell $4f$ transitions in Yb^{3+} ions in lithium niobate crystals*, Physical Review B: Condensed Matter and Materials Physics **72**(22), 2005, pp. 224104-1–5.
- [53] TAKEMURA K., SYASSEN K., *High pressure equation of state of rubidium*, Solid State Communications **44**(8), 1982, pp. 1161–4.
- [54] KUNTSCHER C.A., FRANK S., LOA I., SYASSEN K., YAMAUCHI T., UEDA Y., *Infrared properties of the quasi-one-dimensional superconductor $\beta-Na_{0.33}V_2O_5$ under pressure*, Physical Review B: Condensed Matter and Materials Physics **71**(22), 2005, pp. 220502-1–4.
- [55] MACFARLANE P.I., HOLLIDAY K., NICHOLLS J.F.H., HENDERSON B., *Characterization of Cr^{3+} centres in $LiNbO_3$ using fluorescence line narrowing*, Journal of Physics: Condensed Matter **7**(49), 1995, pp. 9643–56.
- [56] GRACHEV V., MALOVICHKO G., *EPR, ENDOR, and optical-absorption study of Cr^{3+} centers substituting for niobium in Li-rich lithium niobate crystals*, Physical Review B: Condensed Matter **62**(12), 2000, pp. 7779–90, and references therein.
- [57] BIERNACKI W., KAMIŃSKA A., SUCHOCKI A., ARIZMENDI L., *Nephelauxetic effect in $LiNbO_3:Cr^{3+}$ crystals*, Applied Physics Letters **81**(3), 2002, pp. 442–4.
- [58] SUCHOCKI A., BIERNACKI S.W., KAMIŃSKA A., ARIZMENDI L., *Nephelauxetic effect in luminescence of Cr^{3+} -doped lithium niobate and garnets*, Journal of Luminescence **102–103**, 2003, pp. 571–4.
- [59] GRINBERG M., FELICI A.C., PAPA T., PIACENTINI M., *Nonradiative processes in the $Zn_{1-x}Co_xSe$ system*, Physical Review B: Condensed Matter **60**(12), 1999, pp. 8595–601.
- [60] MONTOYA E., SANZ-GARCIA J.A., CAPMANY J., BAUSA L.E., DIENING A., KELLNER T., HUBER G., *Continuous wave infrared laser action, self-frequency doubling, and tunability of $Yb^{3+}:MgO:LiNbO_3$* , Journal of Applied Physics **87**(9), 2000, pp. 4056–62.

- [61] CHÉNAIS S., DURON F., BALEMBOIS F., GEORGES P., BRENIER A., BOULON G., *Diode-pumped Yb:GGG laser: comparison with Yb:YAG*, *Optical Materials* **22**(2), 2003, pp. 99–106.
- [62] STRĘK W., DEREŃ P., JEŻOWSKA-TRZEBIATOWSKA B., *The nature of Cr(III) luminescence in MgAl₂O₄ spinel*, *Journal of Luminescence* **40–41**, 1988, pp. 421–2.
- [63] GARAPON C., MANAA H., MONCORGÉ R., *Absorption and fluorescence properties of Cr³⁺ doped nonstoichiometric green spinel*, *Journal of Chemical Physics* **95**(8), 1991, pp. 5501–12.
- [64] JASSEMNEJAD B., SUCHOCKI A., POWELL R.C., STRĘK W., DEREŃ P., *Optical spectroscopy and light-induced gratings in Cr³⁺ doped non-stoichiometric magnesium spinel*, *Chemical Physics* **165**(1), 1992, pp. 147–54.
- [65] DEREŃ P.J., MALINOWSKI M., STRĘK W., *Site selection spectroscopy of Cr³⁺ in MgAl₂O₄ green spinel*, *Journal of Luminescence* **68**(2–4), 1996, pp. 91–103.
- [66] GARAPON C., BRENIER A., MONCORGÉ R., *Site-selective optical spectroscopy of Cr³⁺ doped non-stoichiometric green spinel MgO-2.6Al₂O₃*, *Optical Materials* **10**(3), 1998, pp. 177–89.

Received December 15, 2006